Geochemical Study of Natural CO2 Emissions in the French Massif Central: How to Predict Origin, Processes and Evolution of CO2 Leakage

A. Battani, E. Deville, J.L. Faure, E. Jeandel, S. Noirez, E. Tocqué, Y. Benoit, J. Schmitz, D. Parlouar, P. Sarda, et al.

Oil & Gas Science and Technology – Rev. IFP, Vol. 65 (2010), No. 4, pp. 615-633

DOI: 10.2516/ogst/2009052

Dossier

CO_2 Storage in the Struggle against Climate Change
Le stockage du CO_2 au service de la lutte contre le changement climatique

Geochemical Study of Natural CO_2 Emissions in the French Massif Central: How to Predict Origin, Processes and Evolution of CO_2 Leakage

A. Battani[1], E. Deville[1], J.L. Faure[1], E. Jeandel[1], S. Noirez[1], E. Tocqué[1], Y. Benoît[1], J. Schmitz[1], D. Parlouar[1], P. Sarda[2], F. Gal[3], K. Le Pierres[3], M. Brach[3], G. Braibant[3], C. Beny[3], Z. Pokryszka[4], A. Charmoille[4], G. Bentivegna[4], J. Pironon[5], P. de Donato[5], C. Garnier[5], C. Cailteau[5], O. Barrès[5], G. Radilla[5] and A. Bauer[5]

1 Institut français du pétrole, IFP, 1-4 avenue de Bois-Préau, 92852 Rueil-Malmaison Cedex - France
2 Université Paris 11 – Orsay, 91405 Orsay Cedex - France
3 Bureau de Recherches Géologiques et Minières (BRGM), 3 avenue Claude-Guillemin, 45060 Orléans Cedex 2 - France
4 Institut National de l'Environnement Industriel et des Risques (INERIS), Parc Technologique ALATA, 60550 Verneuil-en-Halatte - France
5 Institut National Polytechnique de Lorraine (INPL), 54500 Vandœuvre-lès-Nancy - France

e-mail: anne.battani@ifp.fr - eric.deville@ifp.fr - j-luc.faure@ifp.fr - elodie.jeandel@ifp.fr - sonia.noirez@ifp.fr - eric.tocque@ifp.fr yves.benoit@ifp.fr - julien.schmitz@ifp.fr - daniel.parlouar@ifp.fr - philippe.sarda@u-psud.fr - f.gal@brgm.fr - k.lepierres@brgm.fr m.brach@brgm.fr - g.braibant@ifp.fr - c.beny@brgm.fr - zbigniew.pokryszka@ineris.fr - arnaud.charmoille@ineris.fr gaetan.bentivegna@ineris.fr - jacques.pironon@g2r.uhp-nancy.fr - philippe.de-donato@ensg.inpl-nancy.fr christophe.garnier@ensg.inpl-nancy.fr - cristelle.cailteau@ensg.inpl-nancy.fr - odile.barres@ensg.inpl-nancy.fr giovanni.radilla@mines.inplnancy.fr - allan.bauer@ensg.inpl-nancy.f

Résumé — Étude géochimique des émissions naturelles de CO_2 du Massif Central : origine et processus de migration du gaz — Cette étude présente les principaux résultats de campagnes de monitoring géochimique menées en 2006 et 2007 dans le cadre du projet Géocarbone-Monitoring, sur le site de Sainte-Marguerite, situé dans le Massif Central. Ce site constitue un « laboratoire naturel » pour l'étude des interactions CO_2/fluides/roches et des mécanismes de migration du CO_2 vers la surface, à l'échelle des temps géologiques. Le caractère particulièrement émissif de cet « analogue » permet également de tester et valider des méthodes de mesure et de surveillance des futurs sites de stockage de CO_2. Au cours des campagnes de terrain, nous avons analysé des flux de CO_2 entre le sol et l'atmosphère, et nous avons prélevé et analysé à la fois des gaz des sols, et du gaz provenant de sources carbo-gazeuses, présentes dans toute la région. Un dispositif de « monitoring continu » dans le temps a également été testé, afin d'enregistrer conjointement les teneurs en CO_2 de l'atmosphère et dans le sol en un point précis. Nous avons pu mettre au point un suivi géochimique basé sur la composition isotopique des gaz rares prélevés dans les sols. L'ensemble de nos résultats, confronté à la géologie de terrain, nous a permis de mettre en évidence l'origine mantellique du CO_2. Ce CO_2 remonte rapidement à la surface à l'état gazeux, le long de failles normales et/ou décrochantes, actives actuellement. Les teneurs et flux de CO_2 dans le sol sont spatialement variables et élevés, et montrent également une origine mantellique. Les teneurs atmosphériques semblent faiblement augmenter par rapport à l'important dégazage observé dans la région.

Abstract — Geochemical Study of Natural CO_2 Emissions in the French Massif Central: How to Predict Origin, Processes and Evolution of CO_2 Leakage — *This study presents an overview of some results obtained within the French ANR (National Agency of Research) supported Géocarbone-Monitoring*

research program. The measurements were performed in Sainte-Marguerite, located in the French Massif Central. This site represents a natural laboratory for CO_2/fluid/rock interactions studies, as well as CO_2 migration mechanisms towards the surface. The CO_2 leaking character of the studied area also allows to test and validate measurements methods and verifications for the future CO_2 geological storage sites. During these surveys, we analyzed soil CO_2 fluxes and concentrations. We sampled and analyzed soil gases, and gas from carbo-gaseous bubbling springs. A one-month continuous monitoring was also tested, to record the concentration of CO_2 both in atmosphere and in the soil at a single point. We also developed a new methodology to collect soil gas samples for noble gas abundances and isotopic analyses, as well as carbon isotopic ratios.

Our geochemical results, combined with structural geology, show that the leaking CO_2 has a very deep origin, partially mantle derived. The gas rises rapidly along normal and strike-slip active faults. CO_2 soil concentrations (also showing a mantle derived component) and CO_2 fluxes are spatially variable, and reach high values. The recorded atmospheric CO_2 is not very high, despite the important CO_2 degassing throughout the whole area.

INTRODUCTION

The Geocarbone-Monitoring research program was proposed to test several measurement technologies and subsequently to elaborate a strategy to monitor future industrial CO_2 storage sites. The success of CO_2 underground geological storage also depends on the CO_2 storage safety, and this leads to develop warning technologies based on monitoring soil gas composition and its evolution through time. Soil or near surface strata gas composition must be verified by several methods. Natural CO_2–bearing fluid seepages are reported and studied in many locations throughout the world (Baines and Worden, 2004; Pearce, 2005; Lewicki *et al*., 2007; Shipton *et al*., 2004, 2005). Though such leaking areas will never be used as a candidate for engineered CO_2 storage, these sites represent natural laboratories for the study of CO_2/fluids/rocks interactions over the long term, providing relevant information for future anthropogenic CO_2 storage, as well as data for numerical predictive models. They also offer the possibility to evaluate the impact of degassing CO_2 on the environment, human health and vegetation. Finally, natural occurrences of CO_2 enable to test and further design appropriate techniques of monitoring for industrial CO_2 storage sites.

In the Geocarbone-Monitoring project, we compare two natural analogues with different behaviour regarding natural CO_2. Results from the Montmiral site, located in the Valence (Drôme) sedimentary basin, are presented and discussed in Gal *et al*. (2009) this volume. Here, we focus on the CO_2 leaking site of Sainte-Marguerite, which belongs to the quiescent volcanic area in the French Massif Central. This site is the location of important natural CO_2 release. It can be compared to numerous sites in Italy (for instance the leaking Latera geothermal field), where some monitoring have been performed with similar aims (Chiodini *et al*., 1998, 2001, 2004; Beaubien *et al*., 2003, etc.).

This paper summarizes the results of one geochemical monitoring survey made in 2007. We also present some results from an earlier survey (2006). Our purpose was to define a methodology of measurements that allow to verify the security of future industrial storage sites, for which we must be able to measure leaks of very different magnitudes (very low to high). We tried also to distinguish between natural background CO_2 variations (such as atmospheric and/or soil respiration variations) and a deep-CO_2 leak. In addition to soil gas monitoring, a continuous CO_2 record was conducted both on the atmosphere CO_2 level and in a 1.5 m-deep borehole, during one complete month.

We attempted to determine the source of the naturally occurring CO_2, both in the bubbling springs and in the soil. We used a combination of $\delta^{13}C$ (CO_2) and noble gases isotopes in each case. We tried also to determine the area of high CO_2 fluxes, as well as areas of high CO_2 concentrations (and some associated tracers like ^{222}Rn activities and helium concentrations) and then, we compared both series of data, to see if they correlate. We then investigated any relationship between the local geology and the leakage pathways. Finally, we suggested a process by which gas is migrating from depth to the surface. The tracer data such as noble gas concentrations (He, Ne, Ar, Kr and Xe) and noble gas isotopic ratios, as well as $\delta^{13}C$ measurements are important tools for identifying the source of gas, as well as physical processes that occurred after their genesis (Battani *et al*., 2000; Ballentine *et al*., 2002 and references herein).

The stable carbon isotopic ratio, noted $\delta^{13}C$, is expressed with reference to the Pee Dee Belemnite (PDB) standard. The biologic sources tend to have isotopically lighter carbon than inorganic sources. The range of measured CO_2 isotopic composition in the soil can be very wide, even in volcanic areas, for instance from 0.73‰ to –33.54‰ in Chiodini *et al*. (2008).

The measured $\delta^{13}C$ of the gas, if it sometimes directly reflects its origin, could however be affected by a post-genetic phenomenon of segregation, probably during the migration (Prinzhofer *et al*., 2000). In volcanic and hydrothermal areas, CO_2 reaching the soil level is mainly

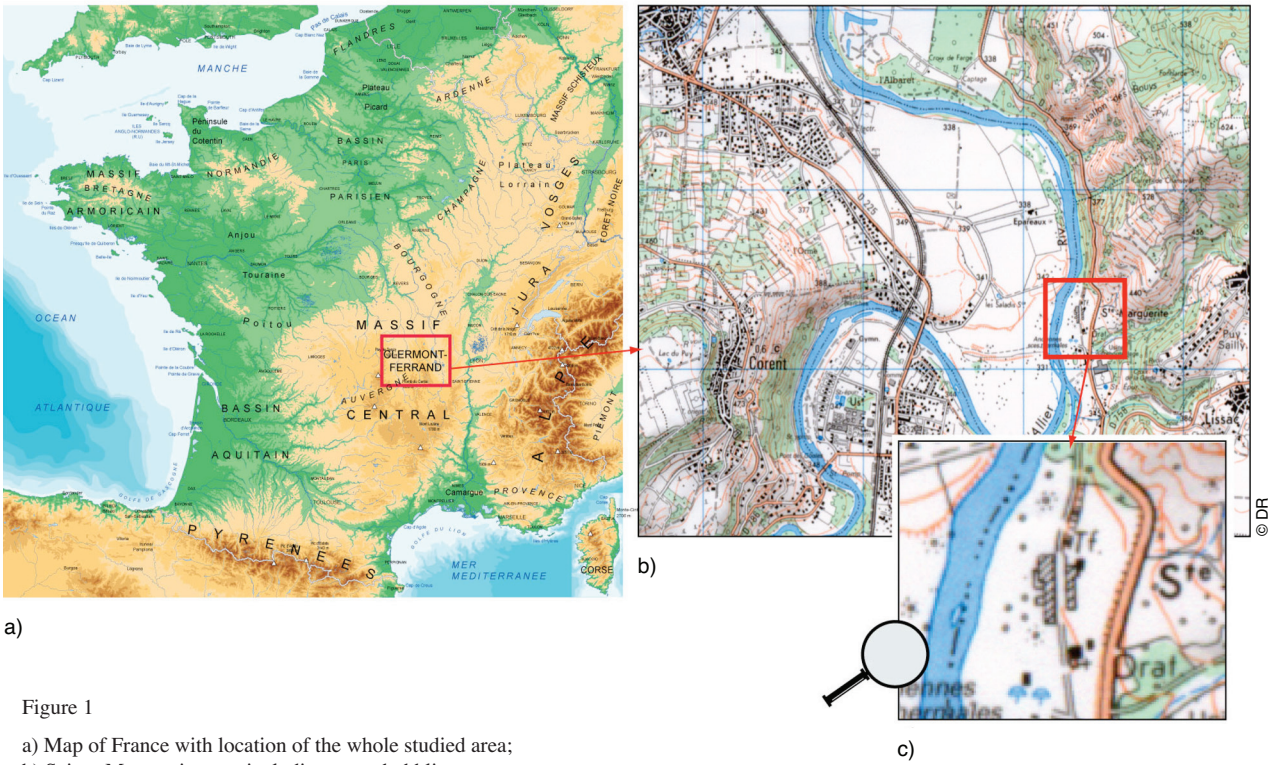

Figure 1

a) Map of France with location of the whole studied area;
b) Sainte-Marguerite area including some bubbling sources;
c) Area of flux and soil gas measurements.

produced by the terrestrial mantle via magma degassing, although another possible source is thermal breakdown of carbonates. CO_2 in soil is also produced by microbial decomposition of organic matter and root respiration. The $\delta^{13}C$ of mantle-derived CO_2 equals $-5.2 \pm 0.7‰$ *vs* PDB (Marty and Zimmerman, 1999). In addition, in natural systems, there is an overlap between $\delta^{13}C(CO_2)$ from the mantle and $\delta^{13}C$ of CO_2 coming from thermal maturation of carbonates rocks (Sherwood Lollar *et al.*, 1997). Because of these different possible sources, as well as the overlapping of $\delta^{13}C$ of deep CO_2 with other sources, we collected samples for helium isotopic measurements in soil gas. Indeed, for other types of samples, noble gases, and more particularly the $CO_2/^3He$ ratio, have shown to be powerful tools to distinguish between thermal decarbonation and magmatic sources of CO_2 (Sherwood Lollar *et al.*, 1997; Ballentine *et al.*, 2002 and references herein).

1 GEOLOGICAL SETTING

The Sainte-Marguerite area is located in the southern part of the Limagne graben, French Massif Central *(Fig. 1)*. The occurrence of many CO_2-rich springs in this area indicates extensive natural emissions of CO_2 *(Fig. 2)*. Most of the

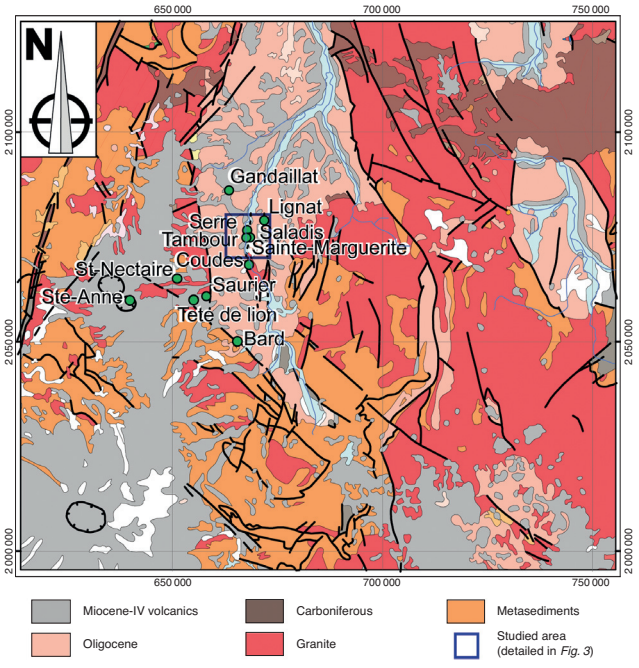

Figure 2

Structural map of the studied area. The sampled bubbling sources are shown in circles.

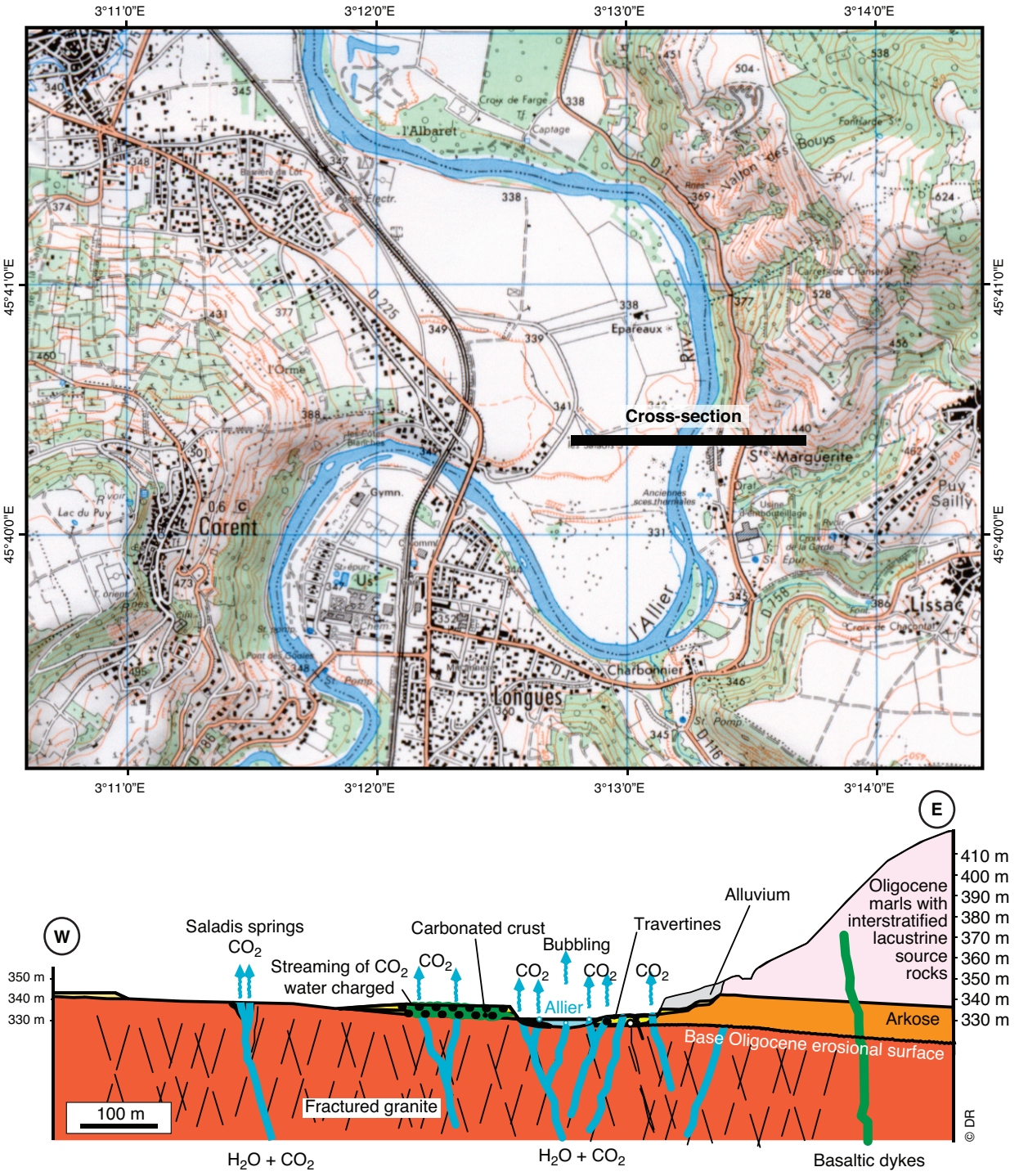

Figure 3

The detailed "Sainte-Marguerite" area and WE geological cross section.

sampled springs are located just above two principal fault systems oriented N10-30 and N110-130, which are certainly inherited from the tardi-Hercynian period (Michon, 2000; *Fig. 2*).

A geological cross-section of the studied area is shown in Figure 3. This area is located at the contact between the Hercynian basement and the transgressive Oligocene marls and limestones. It corresponds to a monocline that gently

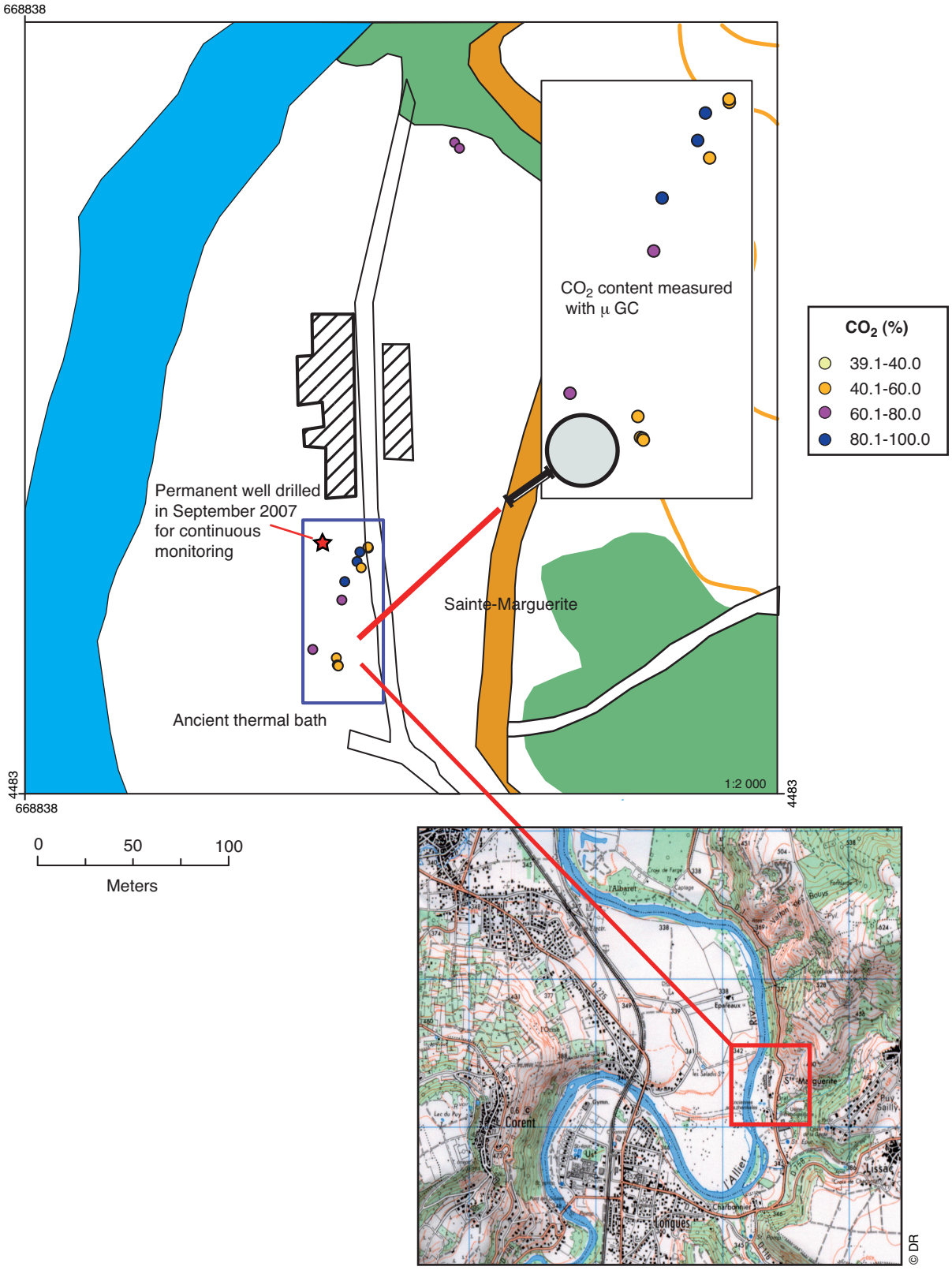

Figure 4

Map from the soil CO_2 (%) gas measurements (with μGC) in the area of an ancient thermal establishment (soil gas and flux survey).

dips about 5° to the east. The basement, made of highly fractured granite, outcrops toward the west of the section, notably around the Saladis spring (cross section, *Fig. 3*).

An intercalated arkosic permeable interval between the fractured granite and the Oligocene marls and limestones may act as a stratiform drain for fluid migration. The overlying thick Oligocene interval is impermeable and acts as a seal, and so may drive the fluid trough the arkose interval toward the Sainte-Marguerite area.

The Allier-river bed is located around the contact between the basement and the sedimentary rocks (see *Fig. 3*). The solid fraction transported by the river has formed several fluvial terraces *(Fig. 3)*.

The Sainte-Marguerite area is also known for the travertines deposits associated with the emergence of CO_2-rich natural springs (Rihs *et al*., 2000). The precipitation of the travertines occurred both in the granite outcrops where the springs are located, and in the fluvial terraces of the Allier-river, where fluid seepages are also observed.

2 METHODOLOGY FOR SAMPLING AND ANALYSIS

2.1 Location of the Different Sampled Areas

The investigated area for the soil gas measurements was chosen around an ancient thermal bath *(Fig. 4)*, where we performed direct soil gas composition measurements. For sampling of the CO_2-rich sparkling springs, gas was collected in a much larger area (see *Fig. 1* and *2*), where numerous bubbling springs are known. Soil gas samples were also collected for subsequent noble gas and $\delta^{13}C$ isotopic analysis in the laboratory.

2.2 Direct or on-Site Soil Gas Measurements

2.2.1 The "Micro" Gas Chromatograph and Portable Infrared Techniques

The concentrations of major soil gases (C_1 to C_5, CO_2, N_2, H_2, O_2,) were measured in the field by gas chromatography using a Varian© portable micro chromatograph *(Fig. 5)*, equipped with three columns and a Thermal Conductivity Detector (TCD). The probes are stainless steel tubes with sampling holes drilled within the conic shaped end of the tubes. They are driven into the ground, at a depth of about 70 to 90 cm to avoid atmospheric contamination and major influence of meteorological variables (Beaubien *et al*., 2003). Analyses are performed in a few minutes and repeated several times to control any air contaminating the system. Measurements where also carried out in the atmosphere to verify the calibration of the chromatograph.

Determination of soil gas species was also done on-site with portable Infra Red Gas Analysers (IRGA). Both the

Figure 5

The Varian© "Micro" Gas Chromatograph in acquisition. Pictures of the sampling containers (and their connexion to the μGC) for laboratory measurements at the bottom.

LFG20 (*ADC Gas Analysis Ltd*.) and GA2000 (*Geotechnical Instruments Ltd*.) were used to determine CO_2, CH_4 and O_2 concentrations. Sampling was done after drilling a small hole within the soil (c.a. 1 m depth, 1 cm in diameter) using a battery-powered drill and inserting a copper tube (1.10 m long) into the hole. This copper tube is not fully lowered into the soil, to avoid risks of 1) water fill in if the soil is near saturation, or 2) closing of the inner part of the tube by soil particles. Risk of atmospheric contamination can be discarded as isotopic results do not show any kind of contamination in the following cases: 1) no depletion of atmospheric components in the case of drilling in CO_2-rich areas (CO_2 of deep origin); 2) no enrichment of atmospheric components in areas dominated by CO_2 production under biological processes, even if the CO_2 content is as low as hundreds of ppm (see Gal *et al.*, 2009, this volume). Moreover, as the used drill has the same diameter than the copper tube, the residual risk of contamination that could eventually exist is the same than for hand hammer percussion. Indeed, such a process creates vibrations into the soil that can also lead to a non-perfect fitting along the soil column, and sampling of a mixture of gas of different levels.

Internal calibration of this sampling method has been conducted, with reproducibility and results being equivalent to those recorded using stainless steel probes progressively lowered down into the soil by hand-hammer percussion. Particular attention was taken to properly seal the copper tube, to avoid leaks and atmosphere contamination. The copper tube is then connected to the IRGA, where pumping is done at a low flow rate (200 $mL.min^{-1}$). Equilibration of the gas concentration occurs within one or two minutes, then values are recorded. The LFG20 detection limits are 0.05% with a precision of ±0.5% between 0 and 10% CO_2, ±3% between 10 and 50% CO_2 and ±5% above. For the GA2000, the precision is ±0.5% between 0 and 5% for CO_2 and CH_4, ±1% between 5 and 15% and ±3% above. Calibrations of the IRGA were done in the laboratory and verified on site by using CO_2 standards at 0.05, 10.2 and 100% CO_2.

As pointed out in this paragraph, intercomparison with hand-hammered methods has led to very similar results. Moreover, tests have shown that the principal cause of CO_2 content variation using this method is not the depth reached by the copper tube, but rather the depth reached by drilling. At Sainte-Marguerite (see *Sect. 3.3.3*) comparative measurements undertaken at 60 and 100 cm depth have shown that reached depth is the key parameter. Variable lowering of the copper tube performed during this acquisition has not led to noticeable variation of the measured CO_2 content. Repeatability assessment, that could be done by inserting - measuring - removing the probe as many times as wanted, also leads to very comparable results if done in a restricted time (to avoid influence of diurnal cycles). This is another evidence of the very limited impact of penetration at depth of atmospheric gas.

The fundamental point using such soil gas sampling method is then to achieve the same depth rather than willing to lower a probe always at the maximum reachable depth. Results shown in this paper were all acquired using this method, so they are significant and can be compared one to the other with a great level of confidence.

2.2.2 Flux Measurements

Directly measuring the gaseous flux in soil/atmosphere interface is one of the most effective way of monitoring a gas emission from the ground. The flux of CO_2 was measured using the accumulation chamber technique (Chiodini *et al.*, 1998). The gas escapes from the covered area then accumulates in the chamber. In this way it is possible to monitor how the atmosphere becomes enriched in the studied gas. A sample of the mixture is fed to an analyser and then returned to the chamber. By monitoring the rate at which the recirculated mixture is enriched in the gas, it is possible to deduce the local gas flow at the given point. The dimension of the chamber and the operating parameters of the method were optimised at the design stage on a test rig using known gas flows (Pokryszka and Tauziède, 2000).

The measurement system used is relatively simple to operate. The total time necessary for an individual measurement is on the order of 5 to 10 minutes, so that a large number can be made daily (from 30 to over 60 points according to the site accessibility). The exact procedures involved in this method are protected by an European patent (No. 96-05996, filed on May 14th 1996 and entitled "Measurement of gas flows through surfaces"). It allows the detection and quantification of variable CO_2 gaseous fluxes ranging from 0.05 to 4000 $cm^3.min^{-1}.m^2$.

2.2.3 Continuous Monitoring

A permanent 1.5 m-deep borehole was drilled for continuous gas phase monitoring. It was located 10 m eastward of the old thermal bath on a grass-covered alluvial platform ("star" shown in *Fig. 4*). The well completion *(Fig. 6)* is made of a porous membrane protecting a temperature sensor and a gas line. The diameter of the ceramics is slightly smaller than the diameter of the borehole, creating an open space dedicated to gas collection. Gas comes from the soil and from the open cavity. An inflatable packer was placed on the top of the completion in order to isolate the gas collection volume from the atmosphere. The water pressure into the packer was fixed and maintained at 4 bars. The packer was inflated some minutes after the creation of the borehole.

The completion is linked to a system of gas circulation equipped with a pump. The air, pumped from the soil at a 1 m depth with a rate of 10 mL/min, reaches the IR gas cell and is evacuated towards the atmosphere. The gas entrance is located 30 cm above the bottom of the completion. The IR gas cell is a multipass ®*Bruker* cell with an IR beam length varying from 0.25 to 1 m. The gas cell and the Fourier Transform InfraRed (FTIR) spectrometer are equipped with CaF_2 windows, in order to avoid alteration by humidity. The *Bruker®Tensor* spectrometer is composed by one interferometer, one IR spring and two compartments with two Deuterated TriGlycine Sulfide (DTGS) detectors. One compartment is dedicated to the analysis of gases from the borehole into the soil, the other allows open path recording of the atmospheric gases in a room of the thermal bath. The room is open to the atmosphere and the spectrometer is located 4 m above the soil surface. Infrared spectra are recorded between 5500 and 900 cm^{-1} during 1 minute (20 scans) with a spectral resolution of 2 cm^{-1}. Temperature of the atmosphere and gas pressure into the gas cell are continuously recorded.

Gas concentrations were calibrated in the laboratory from several known gas mixtures at various partial pressures of CO_2 and bulk gas pressures using the three vibration bands of CO_2 located at 2350 cm^{-1}, 3609 cm^{-1} and 4984 cm^{-1}. Spectra of soil gases and of the atmosphere were successively recorded each hour and stored in the hard disk of the computer. Area integrations and recording procedures were

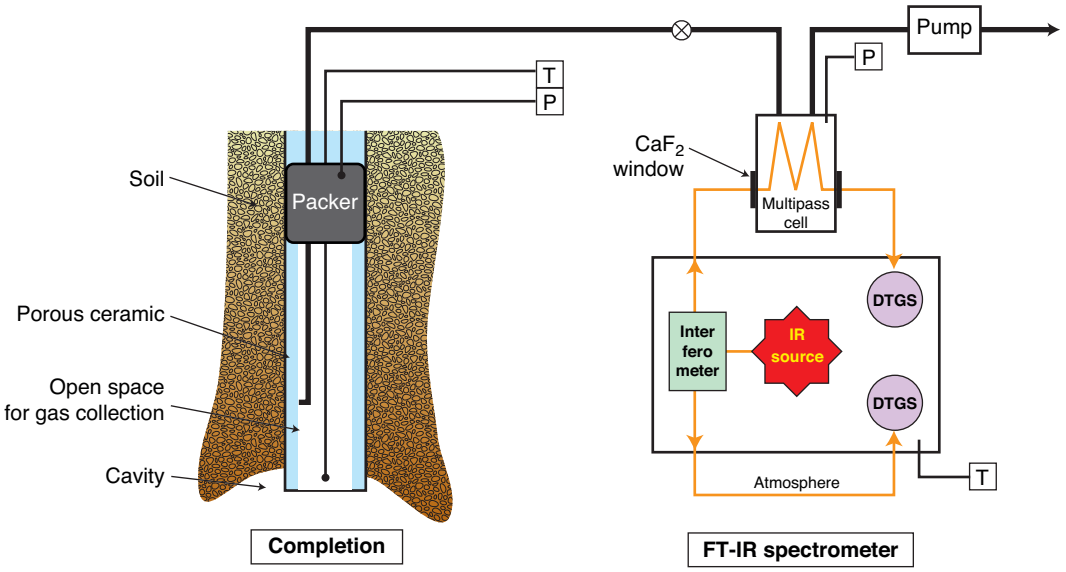

Figure 6

Borehole equipped with a completion coupled to a circulation gas system and a FT-IR spectrometer for on-line CO_2 measurement (*T*: temperature sensor, *P*: pressure sensor).

developed using the ®OPUS software from *Bruker*. Specific quantitative determination procedure of gas concentration has been developed in the laboratory according to the type of IR band used for the CO_2 survey.

The continuous recording covered the period between September the 14th and October the 13th of 2007. This period has been chosen to avoid intense rainfalls and flooding from the Allier-river.

2.2.4 On-Site Soil Gas Tracers Measurements: ^4He, ^{222}Rn

Some samples were collected in order to determine ^{222}Rn activity and helium-4 content. These elements are often associated with naturally occurring CO_2 and are further evidence of fluid origin and/or the presence of faults (deep or shallow). Both belong to the noble gas family, and, therefore, they do not participate to any chemical and biological processes. Moreover, also due to its small size, helium is considered as very mobile and is a good tracer of associated CO_2. Helium concentrations in the soil are commonly given as deviations (positive or negative) relative to the atmospheric level of 5.24 ppm.

For helium abundance measurements, a Tedlar bag is connected to the IRGA, filled and rinsed at least once prior to getting a sample. For radon activity determinations, a vacuum scintillating flask is filled by soil gas (c.a. 200 mL, internal ZnS coating, *Algade*, France).

Helium measurements were performed twice a day, using a modified *Alcatel* leaking mass spectrometer (*Adixen* ASM102S). Sensitivity is 0.1 ppm in the range 0.1 ppm – 100% He.

Radon measurements are done by alpha particles counting (*Calen*, *Algade*) and converted into activity data (Bq/m^3). Alpha photomultiplier background noise is less than 0.2 counts per hour. Counting was done during 180 seconds, stated reproducibility being better than 0.1%.

2.3 Soil Gas Sampling for Laboratory Measurements

A method has been developed and used for the collection of soil gas samples for noble gas abundances and isotopic analyses, as well as carbon isotopic ratios. The samples were collected in pre-evacuated containers of two different types: stainless steel samples fitted with valves all assembled with *Swagelok*® VCR connections (for noble gases, as they are very sensitive to air contamination), while the samples for carbon isotopic ratios were collected in commercially available *vacutainers*®. For all samples, we used the micro-GC as a pump between the stainless steel probe and the sampling containers, to take gas at a one meter depth and purge atmospheric contamination. The different sampling containers and their connexion to the µGC are shown in Figure 5. During sample collection, we checked the decrease of the N_2 and $Ar+O_2$ picks as testimony of atmospheric purge.

Noble gas analyses were subsequently performed using a VG5400 mass spectrometer, devoted to the noble gas abundance and isotopic ratios measurements. The carbon isotopic

ratios were measured with a GC-C-IRMS. Additional samples were collected in vacuum-glass bulbs or stainless steel canisters for laboratory gaseous chromatography measurements (CO_2, Ar, O_2, N_2, CO, He, H_2, H_2S, and light hydrocarbons) and further isotope ratio determination ($\delta^{13}CO_2$ ‰ PDB).

2.4 Sampling from the CO_2-rich Springs (*i.e.* Deep Gas)

Noble Gases and $\delta^{13}C$ of the Bubbling Springs

All the sampled springs had a separate gas phase (bubbles seen in each case). We used a glass funnel, connected to a stainless steel sampling system to sample gas seeps. The funnel was submerged into water to avoid any atmospheric contamination during sampling. The gas was allowed to flow into the stainless steel tube for a few minutes to make successive purges, before we closed the two valves sequentially.

For the analysis of the major gases and the carbon isotopic ratios of the different species, the gas was collected in pre-evacuated *vacutainers*®. Noble gases, as they are very volatiles, were collected in *swagelok*® stainless steel cylinders fitted with a high-vacuum valve at each end. Back in the laboratory, samples from stainless steel cylinders were directly connected to the VG5400 mass spectrometer for noble gas analysis.

The *vacutainers*® were used for $\delta^{13}C$ measurements, where gas was taken with a syringe and introduced into the GC-C-IRMS.

3 RESULTS AND DISCUSSION

3.1 Origin of the CO_2 from the Bubbling Springs from $\delta^{13}C$ and Helium Isotopic Ratios

CO_2 (%) and associated $\delta^{13}C$ measurements from GC-C-IRMS are shown in Table 1. Noble gas abundances and isotopic ratios are reported in Tables 2 and 3 respectively. CO_2 represents the major part (almost 100%) of the gas *(Tab. 1)*.

Measured helium isotopic ratios (expressed as R/Ra, where R is the measured $^3He/^4He$ isotopic ratio from the sample, and Ra is the atmospheric $^3He/^4He$ value of 1.4×10^{-6}) range between 0.76 and 6.62 *(Tab. 3)*. This last value is very high, and compares with a pure mantle component (European Sub Continental Mantle (SCM): $R/Ra = 6$ and upper mantle $R/Ra = 8$ (Gautheron and Moreira, 2002 and Kurz and Jenkins, 1981 respectively). In addition, the measured $\delta^{13}C$ in the bubbling springs is around –5‰, typical of mantle-derived CO_2 (Marty and Zimmerman, 1999). We can therefore conclude that an important proportion of CO_2 in this area is mantle-derived (more than 40%, Battani *et al.*, in prep.).

TABLE 1

CO_2 (%), $\delta^{13}C(CO_2)$ and associated error of some of the bubbling springs gas samples

	CO_2 (%)	$\delta^{13}C(CO_2)$	σ
Geyser	98.5	-4.78	0.15
Tête de Lion	97.2	-4.93	0.15
Petit Saladis	99.6	-5.63	0.15
Grand Saladis	99.8	-4.15	0.15
Lagune	100	-4.98	0.15
Lignat 1	100	-4.98	0.15
Allier	98.8	-5.29	0.15

3.2 Transport of CO_2 to the Surface Deduced from the Springs Samples Data

Low Helium Content and Argon Isotopic Fractionations

The helium-4 concentrations range from 0.12 to 39.12 ppm *(Tab. 2)*, with most of the samples having lower helium-4 concentrations than the atmospheric value of 5.24 ppm.

This low content is a surprising result, as the springs emerge from the granitic basement, and should therefore trap excess helium-4, due to the U and Th radioactive decay. This result can only be explained if the fluids migrate very fast from depth to the atmosphere.

A thermodynamic calculation confirms that the fluids migrated as gas phase. Assuming a typical He concentration in MORB (Mid Ocean Ridge Basalt) of 10^{-5} cc STP/g and a solubility constant $K_{He} = 5.6\times10^{-4}$ cc STP/g.bar in a silicate melt (Jambon *et al.*, 1986), a concentration of 3 ppmV of helium-4 is obtained from the degassing of MORB at 25 km depth. The later depth was chosen according to the teleseismic tomography experiments revealing a magmatic body beneath the Fench Massif Central (Granet *et al.*, 1995).

Next, if such a gas dissolves in water at 1 km depth, with a mean T of 75°C (anomaly due to the ascending melt), and a solubility constant of $K_{He} = 1.267\times10^5$ atm/(mol He/mol water) (Clever, 1979) the helium-4 concentration in water should be of 2.2×10^{-9} mol He/mol water, or 2.2×10^{-3} ppmV.

If this water then exsolves CO_2 at the surface (1 bar), we calculate a gas phase with almost 300 ppmV helium-4.

This result is higher than the measured values (0.12 to 39.12 ppmV, *Tab. 2*) and strongly suggests that the CO_2 was not transported from depth by water. We therefore conclude that it was travelling very fast, as gaseous phase. This is different from what was shown in the Colorado plateau (Gilfillan *et al.*, 2008), where the authors studied natural CO_2 reservoirs and showed that most of the CO_2 was dissolved in water at depth before reaching the surface.

The quick transport of the CO_2 gas is also confirmed by argon isotopic fractionation, consistent with a Rayleigh type

TABLE 2

Noble gas analysis from the 2007 survey. Results are given in ppm. Error are given 2sigma

	^{4}He ppm	σ	^{22}Ne	σ	^{36}Ar	σ	^{84}Kr	σ	^{129}Xe	σ
Tambour 1	0.78	0.10	0.0633	0.0079	1.16	0.14	0.025	0.003	0.0005	0.0001
Grand Saladis	2.73	0.34	0.0055	0.0007	0.19	0.02	0.007	0.001	0.0002	3.10^{-5}
Petit Saladis	4.89	0.61	0.0025	0.0003	0.39	0.05	0.024	0.003	<d.l	
Tambour 2	0.87	0.11	0.1169	0.0146	2.29	0.29	0.112	0.014	0.0012	0.0002
Geyser	0.96	0.12	0.0383	0.0048	8.34	1.04	0.623	0.078	0.0062	0.0008
Lignat 2	37.69	4.72	0.0065	0.0008	1.41	0.18	0.119	0.015	0.0014	0.0002
Lignat 1	39.12	4.90	0.0061	0.0008	0.98	0.011	0.090	0.011	0.0013	0.0002
Saurier	0.12	0.01	0.0015	0.0002	0.04	0.00	0.024	0.003	<d.l	
Tête de Lion	2.97	0.37	0.4338	0.0542	4.67	0.58	0.187	0.023	0.0012	0.0001
Ste-Anne	4.35	0.54	0.0074	0.0009	2.35	0.29	0.218	0.027	0.0023	0.0003
Lagune GR	1.61	0.20	0.0026	0.0003	0.07	0.01	0.005	0.001	0.0001	2.10^{-5}
SO23-GR	7.53	0.94	0.9079	0.1135	11.95	1.49	0.393	0.049	0.0045	0.0006
SO15GR	8.81	1.10	0.7395	0.0924	9.47	1.18	0.385	0.048	0.0037	0.0005

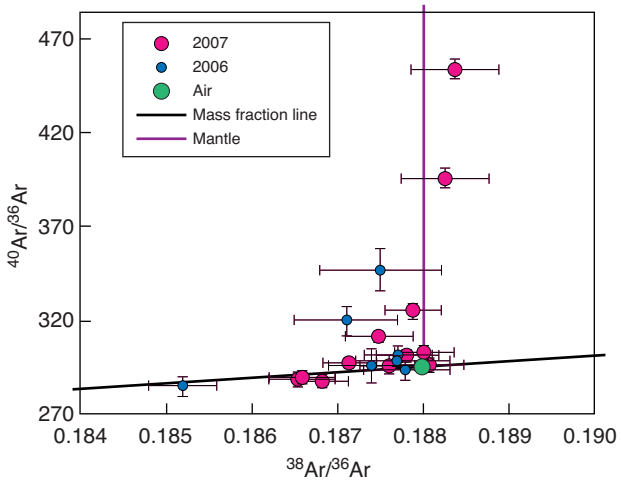

Figure 7

Isotopic fractionation of argon shown in a ^{40}Ar/^{36}Ar *versus* ^{38}Ar/^{36}Ar diagram. Most of the samples (bubbling springs) follow the mass fractionation black line. Increase of some ^{40}Ar/^{36}Ar ratios could either be explained by a mantle derived input, or little addition of radiogenic ^{40}Ar*. This kinetic fractionation indicate rapid migration of the fluid.

process of fractionation. An illustration is given in Figure 7, where Both argon isotopic ratios (^{38}Ar/^{36}Ar and ^{40}Ar/^{36}Ar) follow the Mass Fractionation Line (MLF). Such mass fractionated values are strong arguments for a fast migration process, without any reequilibration. The gas is therefore assumed to migrate fast along the deep-rooted faults of the granitic basement.

TABLE 3

Noble gas isotopic ratios and associated error

	R/*Ra*	σ	^{38}Ar/^{36}Ar	σ	^{40}Ar/^{36}Ar	σ
Tambour 1	2.32	0.52	0.1871	0.0003	297.46	2.23
Grand Saladis 1	3.36	0.47	0.1875	0.0004	311.54	2.37
Petit Saladis	4.27	0.18	0.1879	0.0003	325.05	3.62
Tambour 2			0.1876	0.0004	295.02	3.26
Geyser 100907			0.1876	0.0003	295.02	3.29
Source du Bard			0.1881	0.0004	296.48	3.28
Lignat 2	5.18	0.14	0.1883	0.0004	395.31	4.47
Lignat 1	4.98	0.13	0.1884	0.0005	453.94	5.21
Source du Saurier			0.1880	0.0003	295.95	3.27
Tête de Lion	0.76	0.28	0.1868	0.0003	287.75	3.18
Ste-Anne	5.22	0.38	0.1880	0.0003	303.25	3.37
Lagune	6.62	1.05	0.1878	0.0004	301.31	3.35
SO23GR	2.09	0.11	0.1866	0.0004	289.69	3.21
SO15GR	2.10	0.12	0.1865	0.0003	288.23	3.19

3.3 Results from the Surface Soil and Flux Gas Surveys

3.3.1 Helium Isotopic Ratios: Origin of the CO_2 from the Soil

The soil gas samples revealed the presence of a mantle-derived component. Indeed, as indicated in Table 3 (samples labelled S023GR and S015GR), the helium isotopic ratios are greater than 1 *Ra* (reaching 2*Ra*, where *Ra* is the atmospheric

TABLE 4

Results from gas phase chromatography and $\delta^{13}C(CO_2)$ of soil gas samples

	Ar	N_2	CO_2	O_2	H_2	He	CH_4	C_2H_6	C_3H_8	δC_4	δC_5	δC_6	H_2S	$\delta^{13}CCO_2$
Unit.	%	%	%	%	%	%	%	%	%	%	%	%	%	‰VPDB
SMA-6	0.55	48.4	39.4	12.4	< d.l.	< d.l.	< d.l.	< d.l.	< d.l.	< d.l.	< d.l.	< d.l.	< d.l.	-3.9
SMA-23	0.19	17.5	77.1	4.25	< d.l.	< d.l.	< d.l.	< d.l.	< d.l.	< d.l.	< d.l.	< d.l.	< d.l.	-3.9
SMB-3	0.82	69	12.6	17.9	< d.l.	< d.l.	< d.l.	< d.l.	< d.l.	< d.l.	< d.l.	< d.l.	< d.l.	-3
SMB-11	0.3	26.6	65.8	6.02	< d.l.	< d.l.	< d.l.	< d.l.	< d.l.	< d.l.	< d.l.	< d.l.	< d.l.	-4.8
SMC-8	0.22	18.5	74.7	4.84	< d.l.	< d.l.	< d.l.	< d.l.	< d.l.	< d.l.	< d.l.	< d.l.	< d.l.	-4.7
"Travertine" well	0.002	0.13	97.7	0.023	< d.l.	< d.l.	< d.l.	< d.l.	< d.l.	< d.l.	< d.l.	< d.l.	< d.l.	-5.1
SMD-25	0.43	41.3	49	10.6	< d.l.	< d.l.	< d.l.	< d.l.	0.0025	0.0014	< d.l.	< d.l.	< d.l.	-3
SMD-57	0.31	29	61.9	7.02	< d.l.	< d.l.	< d.l.	< d.l.	< d.l.	< d.l.	< d.l.	< d.l.	< d.l.	-3.7
SMD-75	0.73	59.1	22.5	15.7	< d.l.	< d.l.	< d.l.	< d.l.	< d.l.	< d.l.	< d.l.	< d.l.	< d.l.	-4.8
Detection limit	0.001	0.001	0.001	0.001	0.005	0.005	0.0002	0.0002	0.0002	0.0004	0.0002	0.0002	0.005	

$^3He/^4He$ ratio of 1.4×10^{-6}), indicative of the presence of a mantle-derived component invading the soil, partially diluted compared to the deep component.

This deep component explains the sometimes very high values reached by the CO_2 concentration in the soil. It is very unlikely that such high level could be reached in other type of CO_2 storage, natural or engineered.

3.3.2 Results from $\delta^{13}C$, ^{222}Rn, Noble Gases Abundances

The $\delta^{13}C$ of the soil gas samples range between –3 and –4.8‰, compatible with crustal or mantle origin. One deep sample (c.a. 30 m depth) (labelled "travertine well" in *Tab. 4*) exhibits a $\delta^{13}C$ value of –5.1‰, closer to the mantle-derived CO_2, and CO_2 from the bubbling springs. A possible interpretation for the relative heavier $\delta^{13}C$ of the soil sample compared to the deep ones could be an interaction with the local travertines, which have a $\delta^{13}C$ signature between 4.38 and 7.4‰ (Casanova *et al.*, 1999). Moreover, thermal breakdown of travertine should also explain the high $CO_2/^3He$ ratios from the bubbling springs (sometimes higher than mantle-derived ratios in the range 10^9-10^{10}, (Marty and Jambon, 1987) even if the mantle-derived CO_2 represents more than 40% of the total CO_2). This hypothesis will be further discussed elsewhere.

This interaction between soil gas and travertine is consistent with the measured ^{222}Rn activity, as soil atmosphere in its vicinity (*i.e.* above travertine deposits) experienced activities up to 2×10^6 Bq/m^3. Travertines are considerably enriched in uranium and thorium (between 300 and 10000 times; Casanova *et al.,* 1999), while ^{222}Rn activity is very low for the 30 m-deep well.

In the soil gas samples, gas chromatography measurements allow the detection of argon, with significantly lower amounts than in the atmosphere (0.93%). Taking into account the deep origin for the main gas phase, this relative depletion could be attributed to different levels of mixing, a small amount of argon suggesting a greater proportion of the deep gas flux.

One sample (SMD-25) showed the presence of propane and butane. The total amount is close to 25 ppm and can be related to the presence of bitumen sedimentary series with the Limagne d'Allier graben (Kleinschrod, 1837, Pierre Thomas, personal communication).

The spatial distribution of Rn activity is shown in Figure 8. If we take into account the structural scheme of the area, we can conclude that the preferential pathways followed by the deep gases for migration to the surface is located along a NE-SW trend.

3.3.3 CO_2 Concentrations and Associated Variations of ^{222}Rn and ^4He

A map is shown in Figure 4 with the microGC results. We observe that the CO_2 content is very variable, even for very closely sampled places. The CO_2 content ranges from 40 to 100%. These very high values show an important heterogeneity in distribution. This heterogeneity has also been noticed using the portable IR technique (*Fig. 8* and *9*). In the latter case, soil gas sampling was done at one meter depth to reduce atmospheric contamination (*e.g.* Beaubien et *al.*, 2003). For example, a comparison was done in 2007 along one profile, by taking soil gas respectively at 60 cm and 100 cm depth. For the CO_2 phase, an enrichment ranging between 3 and 30% was obtained for the deepest sample, highlighting the necessity to make measurements always at the same depth.

The monitoring objectives of the 2006 and 2007 surveys were quite different. The first sampling period was devoted to a global site characterisation, with measurements inside and outside the former hydrothermal establishment. The second one focussed on the so identified abnormal zones, in

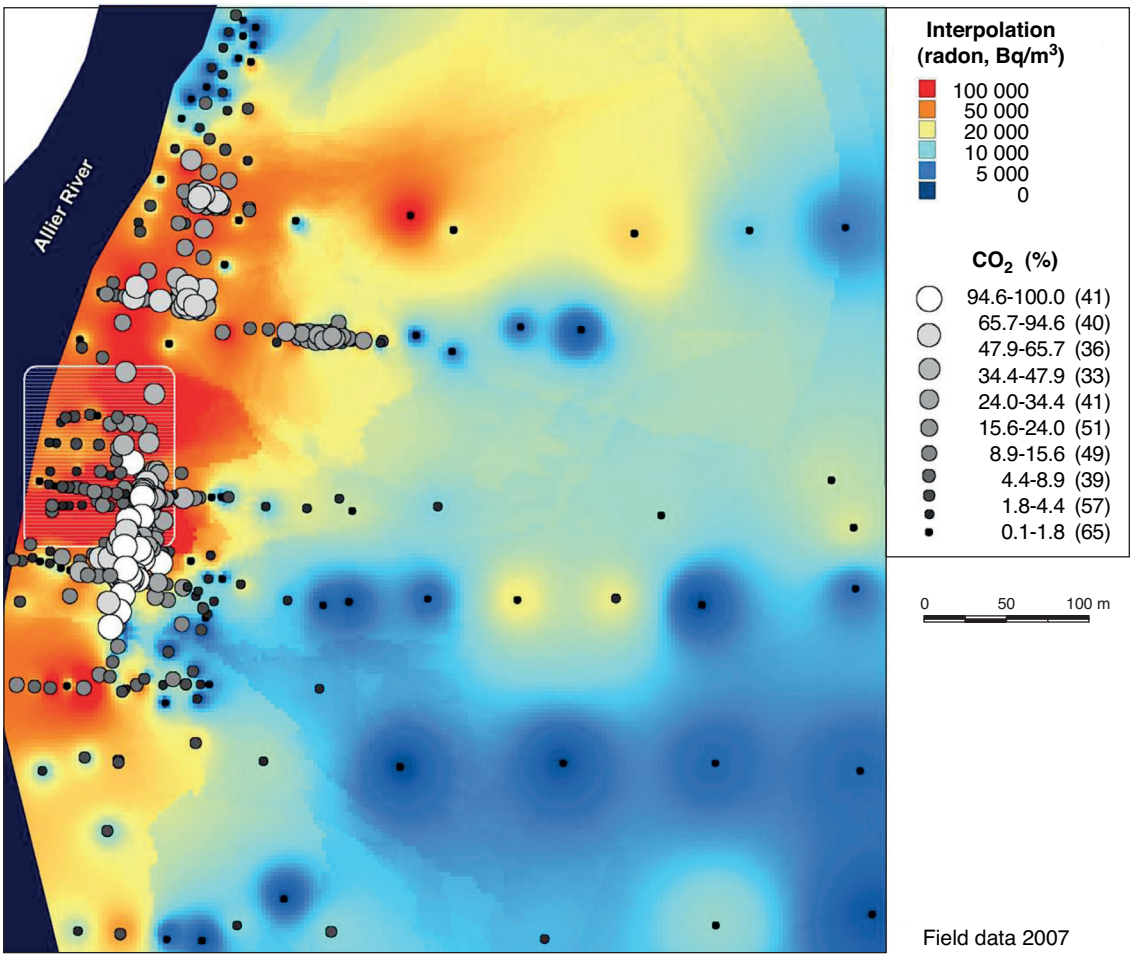

Figure 8

Soil CO_2 (%) content plotted over mean radon activity (Bq/m^3) (2007 survey). Interpolation is done under MapInfo software using the Inverse Distance Weighting function; cell size is 2.6 m and cell influence is 260 m. If two values or more fall within the same cell, then the computed value is the mean. White stripped square: location of massive travertines deposits.

order to better describe their behaviour. As a consequence, mean values are higher in 2007 than in 2006: respectively 38.3% and 10.8% for CO_2, 138 150 and 107 610 Bq/m^3 for ^{222}Rn activities *(Tab. 5)*. Nevertheless, variation ranges are similar, from 0.1 to 100% for CO_2 and from 140 to 2 481 620 Bq/m^3 for radon. This suggests a common mechanism that leads to the existence of soil gas anomalies. A comparison between high values *(Fig. 8)*, *i.e.* greater than 50% for carbon dioxide and 50 000 Bq/m^3 for radon activities, suggests a good agreement between those two gases. As previously mentioned, deep rising CO_2 may interact with deposits enriched in uranium and thorium, especially with superficial travertines (but not with the granitic basement, cf. *Sect. 3.2*) *(Fig. 8)*. Moreover, the CO_2 rising is favoured by the local geology: greater anomalies are aligned along the Allier-river axis (N-S to N20°E), which is related to the former opening of the Limagne graben. High soil gas anomalies should therefore highlight geological structures that do not cross the landscape, but exist under recent sediments. Helium concentrations are more difficult to explain *(Fig. 9)*, as high CO_2 contents can either be linked to low (less than 5 ppm) or high (over 6 ppm) helium values.

3.3.4 CO_2 Fluxes

Figure 10 shows the CO_2 flux measurements made in September 2006 at the Sainte-Marguerite site. The surface

TABLE 5

Statistics

	2006				2007			
	Number of samples	Minimum value	Maximum value	Mean	Number of samples	Minimum value	Maximum value	Mean
CO_2 (%)	131	0.1	97.4	10.8	321	0.17	100	38.3
^{222}Rn (Bq/m^3)	128	329	2481624	107614	180	144	2064122	138150
He (ppm)	131	3.61	6.85	5.18	252	0.99	9.83	5.16

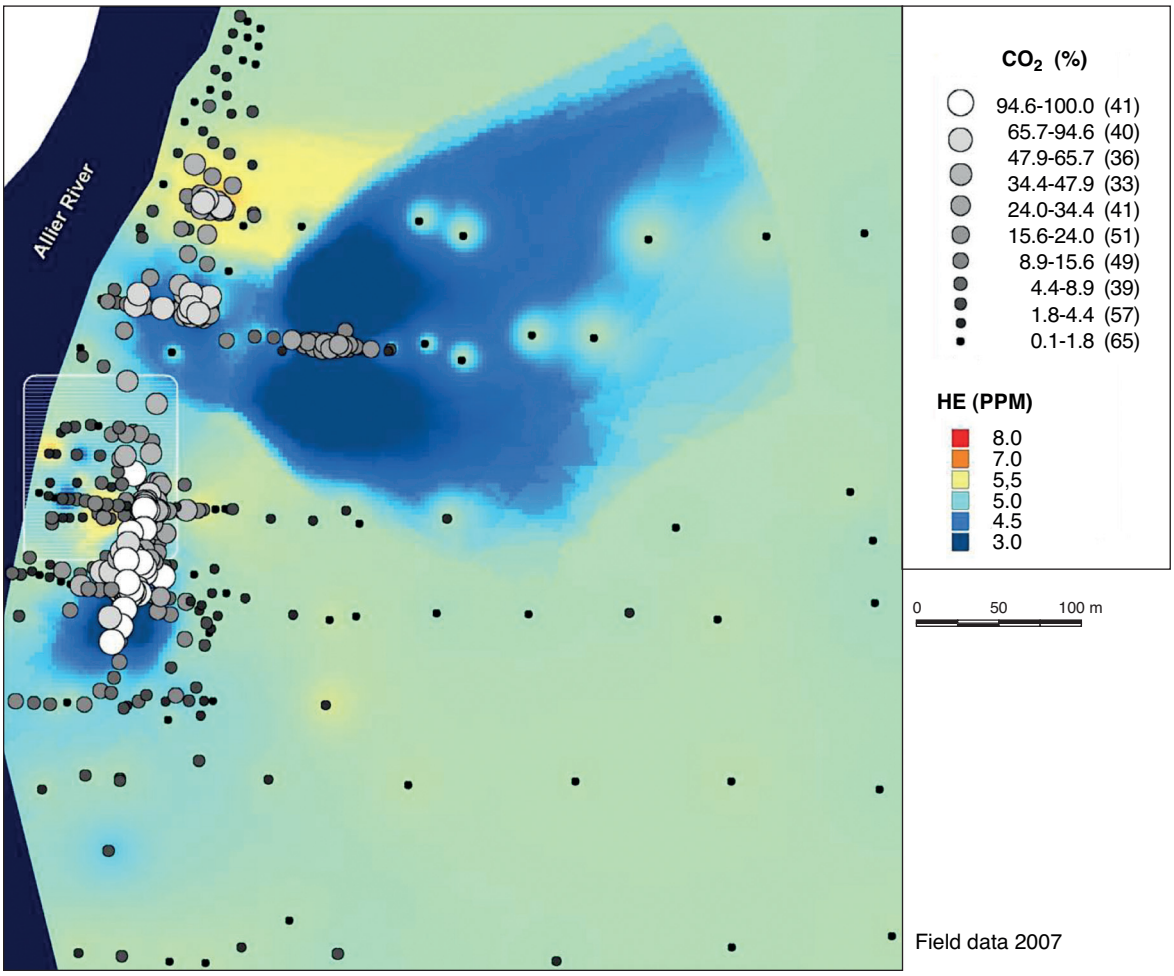

Figure 9

Soil CO_2 content (%) and interpolated content of helium in soil (2007 survey); computation procedure is the same used in Figure 7.

area of the accessible zone covered by the taken measurements is of 5 hectares. The measured flow values range from 1.6 to some 300 $cm^3.min^{-1}.m^{-2}$. The average value obtained from all of the measurements is approximately 35 $cm^3.min^{-1}.m^{-2}$. So as to evaluate the overall flow of CO_2 in the investigated area, we interpolated the measurements using the kriging method. The geographic interpolation illustrated in Figure 11 highlights the presence of two high emissions zones (No. 1 anomaly and No. 2 anomaly).

The first anomaly is located to the North of the former thermal facility hotel (*Fig. 10* and *11*): it extends in the N-S direction and shows its highest values in the southern part.

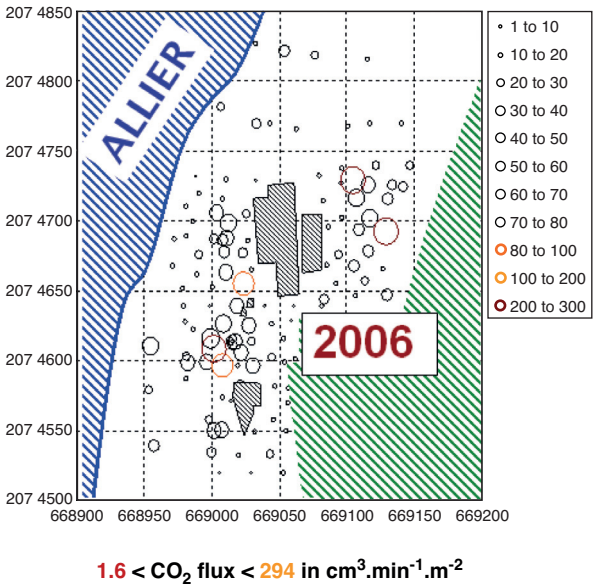

Figure 10

Location and intensity of the CO_2 flux measurements taken in September 2006.

The second is found in the eastern part of the prospected land. This one is less extensive than Anomaly 1, but is characterized by flows that are sometimes greater. The high flux values take on an erratic character and the distribution in space of the CO_2 emissions is more heterogeneous than previously.

By integrating the flow surface presented in Figure 11, we were able to evaluate the overall CO_2 flow rate for the prospected zone. This flow rate is of 1.6 $m^3.min^{-1}$.

The flux measurements taken in 2007 are presented in Figure 12. They are greater than fluxes from 2006. The measured flux values range from 1.2 to some 2800 $cm^3.min^{-1}.m^{-2}$. Anomaly 1, detected in 2006, to the north of the former hotel, with its high emissions levels is still present. In this area, the maximum measured fluxes reach 200 $cm^3.min^{-1}.m^{-2}$. The most important result corresponds to Anomaly 2: it is still present in 2007 but far less marked than in 2006.

The measured fluxes globally reach 2800 $cm^3.min^{-1}.m^{-2}$. The terrains affected by this major flow levels are spatially more extended than in 2006. The characteristics of the emissions in this zone are closer to those of Anomaly 1 with higher maximum values. Geostatistic processing by kriging all the measurements taken in 2007 made it possible to estimate the overall CO_2 flow rate over the prospected zone at 3 $m^3.min^{-1}$.

The measurements taken at the Sainte-Marguerite site showed the presence of significant CO_2 leaking at the surface, with sometimes very high fluxes level of 3000 $cm^3.min^{-1}.m^{-2}$. The average flux value obtained from all the measurements reaches 35 $cm^3.min^{-1}.m^{-2}$ in 2006 and 60 $cm^3.min^{-1}.m^{-2}$ in 2007. For each of the sets of taken measurements, the CO_2 flux exceeds, in a large majority of points, the usual levels of natural emissions of a biological nature by several orders of magnitude (Charmoille *et al*., 2008). In Europe, the maximum CO_2 flux from the ground biological origin ranges between 1 $cm^3.min^{-1}.m^{-2}$ (Jones *et al*., 2005) and 3 $cm^3.min^{-1}.m^{-2}$ (Von Arnold et *al*., 2005). These values were measured on low

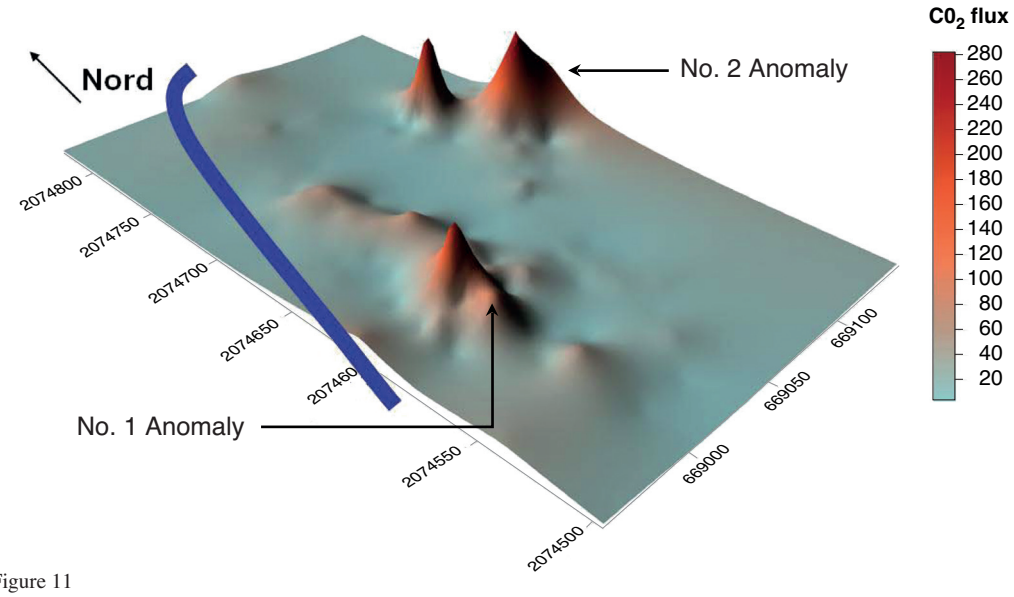

Figure 11

Specialization by kriging the flow of CO_2 at the Sainte-Marguerite experimental site. Measurements taken in September 2006.

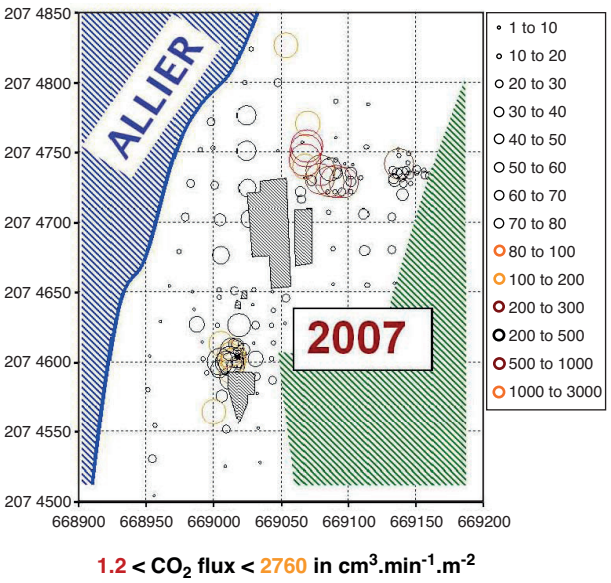

Figure 12

Location and intensity of the measured CO_2 fluxes, taken in September 2007.

lands in clay-sand ground (Scotland) and in leafy forests (birch forests in southern Sweden) respectively.

The CO_2 flows that we measured were therefore clearly of deeper geological origin and are linked to exchanges between the geosphere and the atmosphere. The detected flow anomalies must also correspond to privileged exchange areas facilitated by the geological characteristics of the environment including its permeability.

The spatial structure of the CO_2 flux highlighted in this way *(Fig. 11)* approaches the anomalies described in soil gas concentrations, and is also in good agreement with the results obtained by Baubron *et al.* (1992), from measurements of gas concentrations in the ground (CO_2, Rn, He). The studies previously undertaken at Sainte-Marguerite, especially the hydrogeological surveys ordered by the thermal facility or the bottling plant may help us to interpret the spatial structure of the flows.

Anomaly 1 is located next to the Allier-river, in a zone where the alluvial deposits directly cover the granitic basement. This highly emissive zone is North-South oriented, approaching one of the directions of regional fracturing.

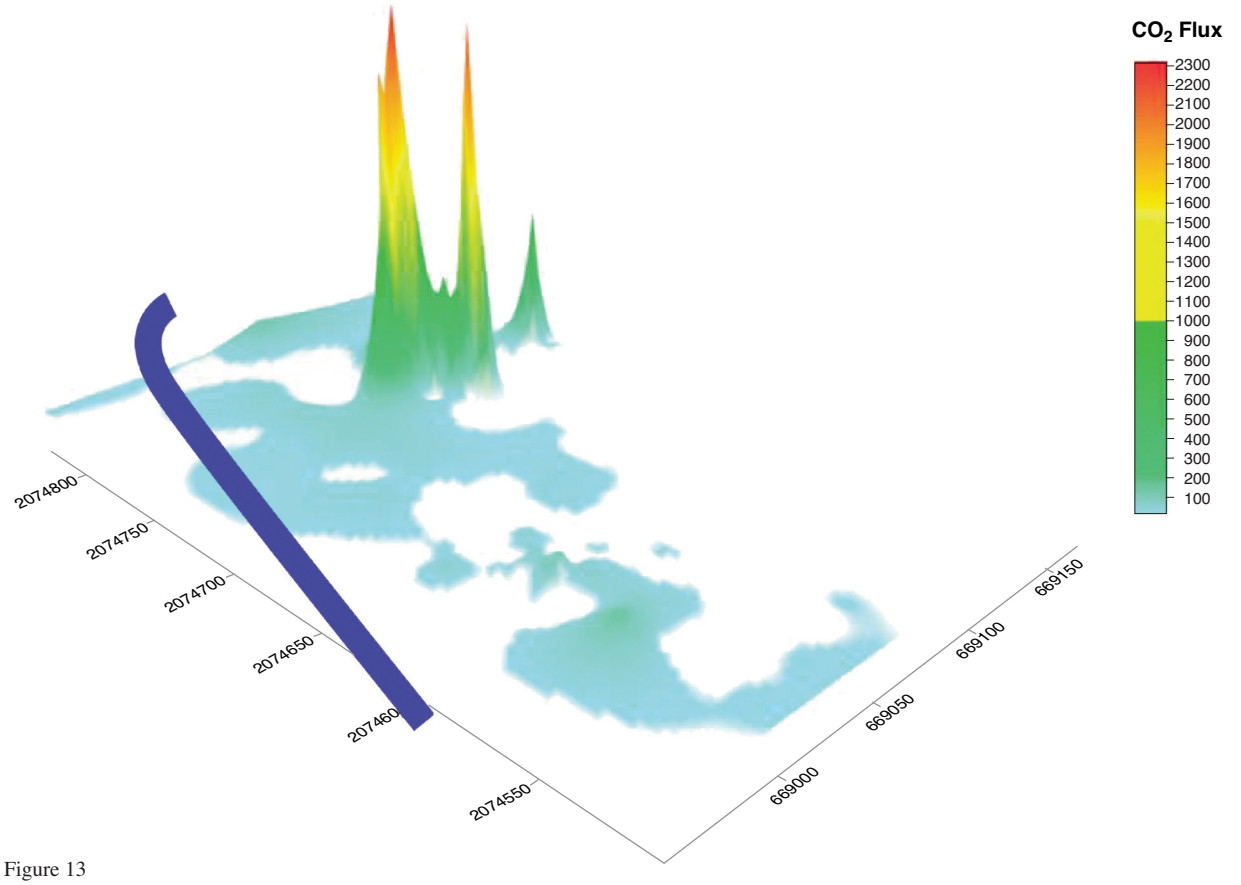

Figure 13

Spatialization of the increase in CO_2 flux levels measured between the 2006 and 2007 measurements.

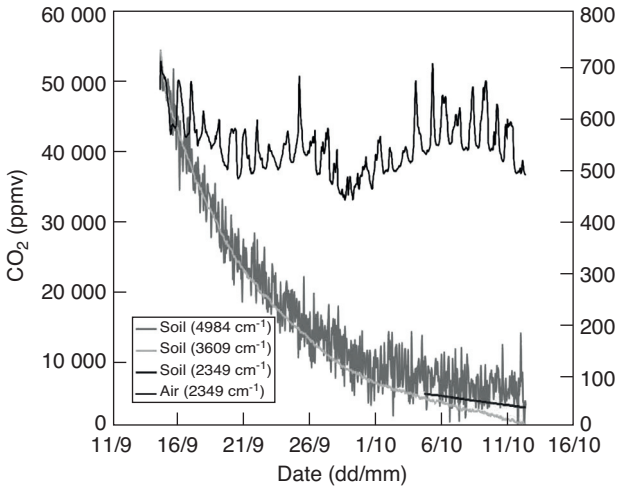

Figure 14

Evolution of the CO_2 content of the atmosphere, at 70 cm above the surface and of the soil at 1.30 m depth from September the 14th to October the 13th of 2007.

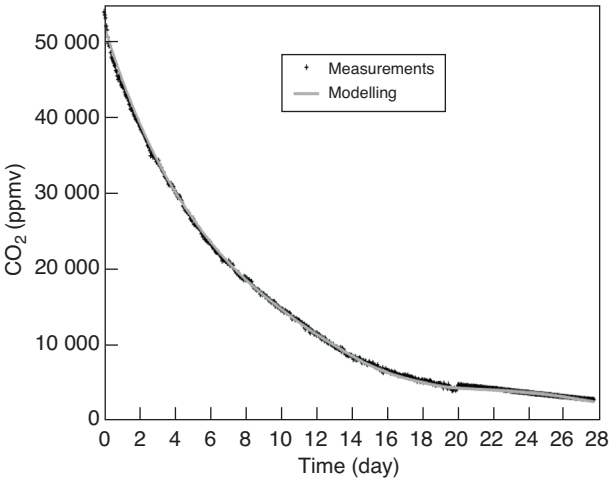

Figure 15

Modelling curve superimposed on the evolution of the concentration of CO_2 at Sainte-Marguerite.

There is a consistency between the alignment of Anomaly 1 and the springs captured to the north of the hotel as well as with the geyser from the Brissac drilling. This North-South direction also corresponds to the limit of the Saint-Yvoine graben.

The Anomaly 2 is a highly emissive zone that was particularly active in 2007. It is located at the intersection between the colluviums and two faults described in Bourgeois and Mercier-Batard (1981): the first fault has a north-south orientation (Anomaly 1) while the second one has an east-west direction. The latter may explain the high fluxes measured around Anomaly 2. These fluxes may also be linked to the presence of a contact between recent alluviums and arkose. This lithological discontinuity constitutes a high permeability zone that allows the migration of CO_2 from soil to surface, as suggested in Figure 13.

The difference between the flow level calculated in 2006 and the one calculated in 2007 is presented in Figure 13. It appears that the most significant rise in the flux level occurred in the "Anomaly 2" area.

A new water pumping point has been opened between the two sets of measurements. The hydrogeological modifications induced by the presence of a drilling for water may be the cause of an increase in the measured flux. Indeed, the well should have linked together permeable intervals that were not originally connected or simply increased the permeability of the crossed formation. Another explanation for the differences between 2006 and 2007 fluxes should be induced by an hydro-climatic impact on subsurface horizons. This is because the water content of the ground may have an influence on its capacity to release gas. Consequently, the wetter the ground, the more impermeable it will be to gas, and *vice versa*.

3.3.5 Continuous Monitoring

Atmospheric and soil CO_2 concentration trends were recorded and are shown Figure 14. Atmospheric CO_2 concentrations determined using the valence band ($v3$) at 2350 cm^{-1} of CO_2 vary from 450 to 700 ppm and show daily fluctuations. The lowest values are recorded early the morning (around 5 am) whereas the maximum CO_2 concentration is reached in the afternoon, around 5 pm. Three sharp peaks are recorded during three different afternoons but their origins cannot be clearly identified. These values are in good agreement with the measured values from the Montmiral area (cf. Gal *et al*., 2009 this volume), strongly suggesting that the maximum value of 700 ppm is essentially due to biological activity.

Soil CO_2 concentrations have been measured using the three vibration bands of CO_2 molecule and drawn Figure 14. Each band has its own validity domain for true determination of gas concentration: lower than 0.5% for the stretching $v3$ vibration centred at 2350 cm^{-1}, between 0.5 and 35% for the combination band ($2v2 + v3$) centred at 3609 cm^{-1} and between 0.7 and 100% for the combination band ($v1 + 2v2 + v3$) centred at 4984 cm^{-1}. The three different curves are more or less superimposed taking into account their own validity domain. Considering the concentration range between 5 and 0.1%, the retained data for the 5-0.5% range are from the combination band located at 3609 cm^{-1} and for data below 0.5% from the stretching band at 2349 cm^{-1} *(Fig. 14)*.

The soil CO_2 concentration shows an exponential-like decrease suggesting that the drilled hole is connected to a cavity containing a constant volume of gas. Indeed, the gas sampled at a constant flow rate is replaced partly by gas coming from the atmosphere and partly by CO_2 coming from a deeper CO_2 source.

A preliminary CO_2 mass balance of the cavity *versus* time showed that it is necessary to take into account the CO_2 concentration fluctuations of the source. Those fluctuations were supposed to be sinusoidal and their period was determined by fitting the model on the experimental data *(Fig. 15)*.

Finally, the concentration of the drilled hole can be described by the following mathematical expression (see *Eq. 1*):

Here, C, C_a, C_{so} and $\tilde{C}_s$ are respectively CO_2 concentration in the drilled hole, in the atmosphere, in the source (mean value) and in the source (fluctuations amplitude). The volume of the cavity is V_o, the gas sampling flow rate is Q_p, parameters ω and Φ are the pulsation and the phase of the source concentration fluctuations, and k is the fraction of the sampled flow rate which is compensated by the atmosphere.

Figure 15 presents results of the modelling, superimposed to the measurements.

The modelling gives the following values: total cavity volume, 210 L; initial cavity concentration, 5.16%; source concentration fluctuations period and phase, 14 days and 4.9 days; fraction of the sampled flow rate compensated by the atmosphere, 98.2%; fraction of the sampled flow rate compensated by the source, 1.8%.

At the scale time of the experiment (one month) these results show that the drilled hole is mainly connected to the atmosphere and very poorly connected to the source of concentration equal to 5.16%. However the initial concentration of the borehole before drilling is not precisely known and was probably higher than 5.16%, due to release towards the atmosphere before the packer was inflated. It can be assumed that the cavity was very poorly connected (or not connected at all) to the atmosphere but connected to a geological source alimented with a CO_2 influx at a very slow rate.

GENERAL CONCLUSIONS AND PERSPECTIVES

Surface soil geochemistry performed in the volcanic-hydrothermal area of Sainte-Marguerite, where natural CO_2 is released to the atmosphere, has shown important and localized CO_2 degassing from depth. In this very emissive area, we did not observe any negative effect on the local vegetation. This could be the result of a progressive adaptation and natural selection of CO_2-resistant species. On the other hand, the atmosphere did not show any anomalous concentration in CO_2 on the period investigated.

We observed good correlations between CO_2 concentrations in soil and CO_2 flux measurements. Both fluxes and concentrations of CO_2 clearly indicate a geological origin, as they are far greater than common biological values. Correlation between the structural geology of the area and the measured geochemical anomalies shows that the faults and fractures are the preferential pathways for gas migration. They affect the granitic basement, and are inherited from Hercynian times (Michon, 2000), but they have been reactivated during Oligocene rifting, and subsequently during the major volcanic phase and uplift from upper Miocene. Today, the region shows an important seismicity (reaching 20 km depth), indicative of permanent fault reactivation.

We noticed important heterogeneities in the spatial distribution of CO_2 concentrations and fluxes in soil during the two geochemical surveys.

CO_2 release to the atmosphere is therefore not only controlled by the presence of faults, but also by more permeable pathways or low-permeability sub-surface layers. These pathways are provided either by fault control on fluid migration, some faults acting as permeable drains, while other act as barriers. On-line gas detection shows that CO_2 is locally concentrated in cavities in the soil, more or less connected to the fault system with CO_2 influx at very slow rate, almost undetectable at the scale of one month of measurement. Atmospheric CO_2 concentration in the studied area records daily variations and some peaks of emission probably related to short periods (less than one hour) of CO_2 release. CO_2 atmospheric concentration is slightly higher than the average atmospheric CO_2 concentration (390 ppm).

Migration of the gas also depends on the more superficial vadose zone and its characteristics (such as lithological variations, water content, etc).

An associated geochemical study of bubbling springs around the Sainte-Marguerite area has highlighted some issues related to the precise origin of the gas, as well as the processes of migration from depth to the surface. The high *R*/*Ra* ratios indicate that the CO_2 has an important mantle-derived contribution. The low helium-4 concentrations indicate that CO_2 is migrating fast and as gaseous phase from depth. The fractionated argon isotopic ratios confirm the rapid migration of the gas from depth.

$$C(t) = \left[kC_a + (1-k)C_{So}\right] + \left(C_O - \left[kC_a + (1-k)C_{So}\right]\right) \exp\left(-\frac{Q_p}{V_O}t\right) + \frac{\tilde{C}_s(1-k)Q_p}{\omega^2 V_O^2 + Q_p^2}\left[Q_p\left(\sin(\omega t+\phi) - \sin(\phi)\exp\left(-\frac{Q_p}{V_O}t\right)\right) - \omega V_O\left(\cos(\omega t+\phi) - \cos(\phi)\exp\left(-\frac{Q_p}{V_O}t\right)\right)\right] \quad (1)$$

This important degassing area enabled to test and integrate several geochemical monitoring methods and to develop and test a methodology for the measurements of noble gas isotopes in soils. This is a strong way to disentangle any deep degassing from biological effects of soil respiration and other biological activity. Repeated measurements of gas flux, associated with soil gas survey gives a precise overview of the leaking character of the site. This is useful for site characterisation, and site monitoring. The addition of new isotopic measurements of the soil gas samples ($\delta^{13}C$ and helium isotopic ratios) is a way to distinguish CO_2 of different origins. Hence, this monitoring technique could be applied to subsurface storage sites, to distinguish between the geochemical signature of injected CO_2 and that of CO_2 naturally present in the shallow subsurface. Such isotopic measurements should also be performed on soil gas samples of the Montmiral area (Gal *et al*., 2009, this volume), which, would give a mean to clearly distinguish between biological CO_2 and CO_2 possibly leaking from the reservoir.

AKNOWLEDGEMENTS

This work was partially supported by the French ANR (National Agency of Research) through the project "Geocarbone-Monitoring". We thank two anonymous reviewers for helping to improve the manuscript. Discussions with R. Deschamps and X. Guichet were very helpful.

REFERENCES

Baines S.J., Worden R.H. (2004) The long term fate of CO_2 in the subsurface: Natural analogues for CO_2 storage, in *Geological Storage of Carbon Dioxide*, Special publication 233, Baines S.J., Worden R.H. (eds.), Geological Society, London, pp. 59-85.

Ballentine C.J., Burgess R., Marty B. (2002) Tracing fluid origin transport and interaction in the crust, in *Noble Gases in Geochemistry and Cosmochemistry*, Reviews in Mineralogy and Geochemistry, 47, Porcelli D.R., Ballentine C.J., Weiler R. (eds), Mineralogical Society of America, Washington DC, pp. 539-614.

Battani A., Sarda P., Prinzhofer A. (2000) Geochemical Study of Pakistani Natural Gas Accumulations Combining Major Elements and Rare Gas Tracing, *Earth Planet. Sc. Lett.* **181**, 229-249.

Baubron J.C., Mercier F., Rouzaire D. (1992) *Eaux de Sainte Marguerite (Puy-De-Dôme) Prospection géochimique in-situ des gaz du sol: Auvergne*, BRGM.

Beaubien S.E., Ciotoli G., Lombardi S. (2003) Carbon dioxide and radon gas hazard in the Alban Hills area (central Italy), *J. Volcanol. Geoth. Res.* **123**, 63-80.

Bourgeois M., Mercier-Batard F. (1981) *Évaluation hydrominérale de Sainte Marguerite (Puy-De-Dôme) : Service géologique régional Auvergne*, BRGM.

Casanova J., Bodénan F., Négrel Ph., Azaroual M. (1999) Microbial control on the precipitation of modern ferrihydrite and carbonate deposits from the Cézallier hydrothermal springs (Massif Central, France), *Sediment. Geol.* **126**, 125-145.

Charmoille A., Pokryszka Z., Bentivegna G. (2008) Développement des méthodes de suivi géochimique en phase gazeuse à la surface des sites de stockage géologique du CO_2, *22e Réunion des Sciences de la Terre*, Nancy, 21-24 avril 2008.

Chiodini G., Cioni R., Guidi M., Raco B., Marini L. (1998) Soil CO_2 flux measurements in volcanic and geothermal areas, *Appl. Geochem.* **13**, 5, 543-552.

Chiodini G., Frondini F. (2001) Carbon dioxide degassing from the Albani Hills volcanioc region, Central Italy, *Chem. Geol.* **177**, 67-83.

Chiodini G., Avino R., Brombach T., Caliro S., Cardellini C., De Vita S., Frondini F., Marotta E., Ventura G. (2004) Fumarolic degassing west of Mount Epomeo, Ischia (Italy), *J. Volcanol. Geoth. Res.* **133**, 291-309.

Chiodini G., Caliro S., Cardellini C., Avino R., Granieri D., Schmidt A. (2008) Carbon isotopic composition of soil CO_2 efflux, a powerful method to discriminate different sources feeding soil CO_2 degassing in volcanic-hydrothermal areas, *Earth Planet. Sc. Lett.* **274**, 372-379.

Clever H.L. (1979) Helium and neon-gas solubility, *Solubility Data Series*, Pergamon Press, Oxford, New York, Toronto, Sydney, Paris, Frankfurt, 1.

Gal F., Le Pierres K., Brach M., Braibant G., Beny C., Battani A., Tocqué E., Benoit Y., Jeandel E., Pokryska Z., Charmoille A., Bentivegna G., Pironon J., de Donato P., Garnier C., Cailteau C., Barrès O., Radilla G., Bauer A. (2009) Surface gas geochemistry above the natural CO_2 reservoir of Montmiral (Drôme-France), source tracking and gas exchange between soil, biosphere and atmosphere, *Oil Gas Sci. Technol. – Rev. IFP* **65**, 635-652.

Gautheron C., Moreira M. (2002) Helium signature of the subcontinental mantle, *Earth Planet. Sc. Lett.* **199**, 39-47.

Gilfillan S.M.V., Ballentine C.J., Holland G., Sherwood Lollar B., Blagburn D., Stevens S., Schoell M., Cassidy M. (2008) Natural CO_2 storage analogues: The noble gas geochemistry of natural CO_2 reservoirs from the Colorado Plateau and Rocky Mountain provinces, USA, *Geochim. Cosmochim. Ac.* **72**, 1174-1178.

Granet M., Wilson M., Achauer U. (1995) Imaging a mantle plume beneath the French Massif Central, *Earth Planet. Sc. Lett.* **136**, 281-296.

Jambon A., Weber H., Braun O. (1986) Solubility of He, Ne, Ar, Kr and Xe in a basalt melt in the range 1250-1600°C. Geochemical implications, *Geochim. Cosmochim. Ac.* **50**, 401-408.

Jones S.K., Ress R.M., Skiba U.M., Ball B.C. (2005) Greenhouse gas emissions from a managed grassland, *Global Planet. Change* **47**, 201-211.

Kleinschrod E.T. (1837) Aperçu géologique sur une partie de l'Auvergne, spécialement sur les environs de Clermont-Ferrand, *Annales scientifiques, littéraires et industrielles de l'Auvergne*, pp. 193-266.

Kurz M.D., Jenkins W.J. (1981) The distribution of helium in oceanic basalt glasses, *Earth Planet. Sc. Lett.* **53**, 41-54.

Lewicki J.L., Birkholzer J.T., Tsang C.-F. (2007) Natural and industrial analogues for leakage of CO_2 from storage reservoirs: identification of features, events, and processes and lessons learned, *Environ. Geol.* **52**, 3, 457-467.

Marty B., Jambon A. (1987) $C/^3He$ in volatiles fluxes from the solid Earth: implications for carbon geodynamics, *Earth Planet. Sc. Lett.* **83**, 16-26.

Marty B., Zimmermann L. (1999) Volatiles (He, C, N, Ar) in mid-ocean ridge basalts: Assessment of shallow–level fractionation and characterization of source composition, *Geochim. Cosmochim. Ac.* **63**, 21, 3619-3633.

Michon L. (2000) Dynamique de l'extension continentale - Application au Rift Ouest-Européen par l'étude de la province du Massif Central, *Thèse Doctorat*, Univ. Clermont-Ferrand.

Pearce J.M. (2005). What can we learn from natural analogues? in *Advances In the Geological Storage of Carbon Dioxide*, Lombardi S., Altunina L.K., Beaubien S.E. (eds), NATO Sciences Series, Berlin, **65**, 129-139.

Pokryszka Z., Tauziède C. (2000) Evaluation of gas emission from closed mines surface to atmosphere, *Environmental Issues and Management Waste in Energy and Mineral Production*, Balkema eds, Rotterdam, pp. 327-329.

Prinzhofer A., Mello M.R., Takaki T. (2000) Geochemical characterisation of natural gas: a physical multivariable approach and its applications in maturity and migration estimates, *Am. Assoc. Petroleum Geol. Bull.* **84**, 1152-1172.

Rihs S., Condomines M., Poidevin J.L. (2000) Long term behaviour of continental hydrothermal systems: U-series dating of hydrothermal carbonates from the French Massif Central (Allier Valley), *Geochim. Cosmochim. Ac.* **64**, 18, 3189-3199.

Sherwood Lollar B., Ballentine C.J., O'Nions R.K. (1997) The fate of mantle-derived carbon in a continental sedimentary basin: Integration of C/He relationships and stable isotope signatures, *Geochim. Cosmochim. Ac.* **61**, 11, 2295-2308.

Shipton Z.K., Evans J.P., Kirchner D., Kolesar P.T., Williams A.P., Heath J. (2004) Analysis of CO_2 leakage through "low-permeability" faults from natural reservoirs in the Colorado Plateau, southern Utah, in *Geological Storage of Carbon Dioxide*, 233, Baines S.J., Worden R.H. (eds.), Geological Society, London, Special Publications, pp. 43-58.

Shipton Z.K., Evans J.P., Dockrill B., Heath J., Williams A., Kirchner D., Kolesar P.T. (2005) Natural leaking CO_2- charged systems as analogs for failed geologic storage reservoirs, in *Carbon Dioxyde CO_2 Capture for Storage in deep Geologic Formations,* Thomas D.C., Benson S.M. (eds), Elsevier, Amsterdam, 2, pp. 699-712.

Von Arnold K., Weslien P., Nilsson M., Svensson B.H., Klemedtsson L. (2005) Fluxes of CO_2, CH_4 and N_2O from drained coniferous forests on organic soils, *Forest Ecol. Manag.* **210**, 239-254.

Final manuscript received in July 2009
Published online in May 2010